



Article

Springback Behavior of Aluminum/Polypropylene/Aluminum Sandwich Laminates

Caroline K. Kella and Pankaj K. Mallick *

Mechanical Engineering, University of Michigan-Dearborn, Dearborn, MI 48128, USA

* Correspondence: pkm@umich.edu

Abstract: The springback of sheet metals after forming has been widely studied for decades using numerical and experimental methods. Many of these springback studies involve aluminum alloys. This study aims to understand the springback behavior of aluminum-polypropylene-aluminum laminates as they are being used increasingly in automotive and other applications because of their weight saving potential. A finite element model of the draw bending of a U-channel based on Numisheet'93 benchmark study is built using LS-DYNA. First, the model is validated and studied for springback prediction of single AA5182-O aluminum alloy sheets, and then it is extended to the study of the springback behaviors of AA5182-O/polypropylene/AA5182-O laminates with various combinations of core and skin thicknesses. The numerical model is also validated by experiment. Effects of various tool design and process parameters, such die radius, punch radius and blank holder force, on the springback of the sandwich laminates are studied. The effect of numerical modeling parameters is also considered.

Keywords: springback; aluminum/polypropylene/aluminum sandwich laminates; draw-bending; numerical modeling



Citation: Kella, C.K.; Mallick, P.K. Springback Behavior of Aluminum/Polypropylene/Aluminum Sandwich Laminates. *J. Manuf. Mater. Process.* **2022**, *6*, 152. <https://doi.org/10.3390/jmmp6060152>

Academic Editors: Chetan P. Nikhare and William J. Emblom

Received: 30 October 2022

Accepted: 21 November 2022

Published: 23 November 2022

Publisher's Note: MDPI stays neutral with regard to jurisdictional claims in published maps and institutional affiliations.



Copyright: © 2022 by the authors. Licensee MDPI, Basel, Switzerland. This article is an open access article distributed under the terms and conditions of the Creative Commons Attribution (CC BY) license (<https://creativecommons.org/licenses/by/4.0/>).

1. Introduction

Springback is a deviation from the die shape that occurs in formed sheet metal parts due to elastic recovery after the forming force is removed and is measured as a change in angles or other dimensional variations. Based on the complexity of the formed geometry, process parameters, material properties and tolerance requirements, it can often be difficult to control this phenomenon. It is considered one of the critical quality control issues in the sheet metal industry.

Processing and design parameters that influence springback of steel and aluminum sheets have been studied for many years. Wagoner et al. [1] reviewed the influence of plastic constitutive equations, variable Young's modulus, through-thickness integration, and different material models on springback. The influence of computational parameters such as integration rule, number of integration points and yield criterion for DC04 steels was studied by Trzepieciniski and Lemu [2], it was observed that the integration rules showed a difference in springback coefficient only when less than five through-thickness integration points were used and the Gaussian integration was closer to the experimental results in comparison to trapezoidal rule. Several studies have been conducted on the influence of material models used for steel and aluminum on springback prediction [3–6] and it is concluded that complex kinematic hardening rules show great improvement in springback prediction but pose difficulty in determining the material parameters. In a study by Hou et al. [7], the three anisotropic yield criteria, Hill48, Barlat89 and Barlat2000 are compared in FE simulation to the experimental yield loci of MP980 obtained through biaxial tension tests. The Barlat2000 model gives the most accurate representation of the yield surface especially for larger plastic strain ranges. The recommendations for accurate prediction of springback in monolithic metals made in the mentioned references is extended to metal-polymer-metal sandwich in this study.

Metal-polymer-metal sandwich laminates are being used increasingly due to their weight saving potential and high flexural stiffness to weight ratio. The mechanical properties and formability characteristics of metal-polymer-metal sandwich laminates have been studied by several researchers [8–11]. In general, the mechanical properties are seen to lie between those of the core and skin layers. Springback of sandwich laminates is a far more complex problem compared to the springback of monolithic sheets, and not much literature is published in this area. Liu and Wang [12] observed that after simple bending, such as V-bending and wiper die bending, metal-polymer-metal laminates exhibit not only a change in the wall angle but also a side-wall curl, whereas monolithic sheets exhibit only a change in the wall angle. They attributed the springback behavior of the laminates to the large difference in the properties of the metal skins and the polymer core in the laminates and proposed an analytical model to predict the springback after laminate bending. According to their model, the springback of a laminate is higher than the springback based on a single layer model given by Gardiner [13]. It is also shown that the springback of a laminate of a given thickness increases with increasing polymer core thickness and decreases with increasing die radius. Ito et al. [14] derived equations for free bending and springback behavior of asymmetric metal-polymer sandwich laminates, assuming that the polymer layer contains only elastic strains. The asymmetry arises from using skins of two different thicknesses. Different cases based on various levels of elastoplastic stress distributions through the thickness of the skins are considered.

Another investigation conducted on steel/polymer/steel panel proposes a model for springback based on 3-point bending experiments by Harhash et al. [15]. The springback angle is defined as the difference between the final bent angle α_f to the initial angle α_i . This model is simple compared to the previously discussed analytical solution and has been validated by experimental results to give reasonably accurate predictions. With varying core thickness value, the effect of the yield strength to modulus (σ/E) ratio of the sandwich laminate is recorded to show that its effect is almost negligible up to a core thickness of 0.6 mm. Increasing the laminate thickness to punch radius ratio leads to smaller springback values. For a constant core thickness, springback increases with increasing bending angle, and for a constant bending angle, springback reduces with increasing core volume fraction. This study also shows a comparison between the experimental and numerical springback values for various core and skin thickness combinations and shows that the finite element model results are close to the experimental values. Results also show that the larger the area of the specimen in contact with the punch radius, the lower is the amount of springback. For asymmetric sandwich laminates, the thicker the steel sheet that was in contact with the punch, the lower is the springback angle irrespective of the core thickness.

Liu and Xue [16] studied the springback behavior of aluminum/polymer/aluminum sandwich laminates in free bending with three different grades of aluminum alloys as the skin material and three different polymers as the core material. It was observed that the springback angle decreases with increasing core thickness and is much higher with the skin material having the highest yield strength compared to that having the lowest yield strength. The core material has much less effect on the springback angle than the skin material. Another study by Ahmed and Chatti [17] compares a semi-analytical model to calculate the springback of steel/polyurethane/steel panels. The polyurethane core was a foam core. Springback was calculated as the difference between the radius of neutral axis before and after unloading. The springback calculated by analytical model shows a decrease as the core thickness increases. However, the experimental and numerical models show a much smaller decrease in springback. Additionally, a simple equation for calculating springback using corrected modulus at large plastic strains is also proposed, and this equation predicts values of springback closer to the experiments. Mohammadi et al. [18] studied the V-die bending of Al3105/polypropylene/Al3105 sandwich sheets. They proposed an analytical model that calculates springback as a sum of the springback in the punch-sheet contact area and springback along the length of the sandwich panel. When compared to numerical and experimental works, the analytical model showed signif-

icantly higher values of springback. Springback in a double curvature stamping operation for aluminum/polypropylene/aluminum sandwiches was studied by Parsa et al. [19] by experimental and numerical methods. In this study, the effects of tool radius and sandwich thickness were considered. Increasing the tool radius showed decrease in springback along both curvature directions. The springback showed an increase with increase in thickness of the sandwich sheet. The effect of mesh strategy and computational model on the springback of HSLA steel/polymer/HSLA steel sandwich material was studied by Solfronk et al. [20]. The Verger yield criterion in combination with isotropic and kinematic hardening laws were compared; use of isotropic hardening showed maximum deviation from experiment. In comparing volume and surface elements for the model using kinematic hardening law, no significant effect on springback was observed. The use of volume elements showed much higher computational time in comparison to surface elements. Springback in a draw-bending process for an aluminum/GFRP/aluminum laminate was examined by Keipour and Gerdooei [21]. The finite element model consists of three separate parts using shell elements that are tied at the interface between the layers. Changing the core layer thickness at constant skin thickness showed minimal effect on springback. Aghchai et al. [22] examined the springback behavior of Al2024/Polyurethane-glass reinforced/Al2024 sandwich laminates using a three-point bending test. The experimental and numerical results are in close agreement. The effects of process temperature, core thickness and rolling direction was studied. By increasing the process temperature, a 22% reduction in springback was obtained and increasing the core thickness showed a 17% decrease in springback.

The published studies on the springback of metal-polymer-metal laminates mostly involve free bending. The current work focuses on the springback behavior of aluminum/polypropylene/aluminum sandwich laminates under draw bending conditions. In draw bending operations, the sheet blank first undergoes bending-unbending deformation around the die corner as it is pulled into the die cavity and then a significant stretching deformation as the final shape of the part is being formed. As the part is released from the die, its sidewalls and flanges exhibit springback due to elastic strain recovery. Additionally, instead of remaining straight, the sidewalls become curved, which is called sidewall curl.

The objective of this research is to determine the springback of AA5182/polypropylene/AA5182 sandwich laminates after draw bending into a U-channel following the Numisheet'93 guidelines. The effect of several skin thickness and core thickness combinations on springback measures, such as wall angle, flange angle and sidewall curl, are considered. Effects of various tool design and process parameters, such die radius, punch radius and blank holder force, on the springback of the sandwich laminates are studied. The effect of numerical modeling parameters is also considered.

2. Materials and Methods

For the purpose of this study, aluminum alloy AA5182-O (annealed) is used as the skin material and polypropylene (PP) is used as the core material to form Al/PP/Al symmetric sandwich laminates. AA5182 is widely used in automotive body panels because of its good formability, corrosion resistance and weldability. The mechanical properties of annealed AA5182-O, henceforth called SA5182, are listed in Table 1.

Table 1. Properties of SA5182 (AA5182-O) [23,24].

Density (kg/m ³)	Modulus of Elasticity (GPa)	Yield Strength (MPa)	Poisson's Ratio	R ₀	R ₄₅	R ₉₀
2890	70	110.2	0.33	0.699	0.776	0.775

Considering the bending and unbending cycle that occurs in the process of forming the U-channel as the material passes over the die radius, the Yoshida–Uemori (YU) hardening model is considered more appropriate to capture the Bauschinger effect more accurately. Although this capability is present in two material models available in LS-DYNA (Mat_226 and Mat_125), Barlat89 yield criterion used in Mat_226 is recommended over Hill48 yield

criterion used in Mat_125 for modelling aluminum alloys [25]. In Numisheet 2005 [26], springback predictions for a crossmember with an aluminum AA5182-O modelled by using Mat_226 show closer values to the experimental results in comparison to Mat_125 and other material models. The aluminum skins in this study are therefore modelled using YU hardening rule combined with Barlat 1989 yield criteria (Mat_226) and the properties for this model are listed in Table 2.

Table 2. Yoshida–Uemori hardening parameters for SA5182 (AA5182-O) [24].

Y (MPa)	R _{sat}	B (MPa)	B (MPa)	h	C	k
110.2	201.7	122.3	16.5	0.16	577.5	12

The polymer in the core is a polypropylene, which has a density nearly one-third that of the aluminum in the skins. The material properties of polypropylene at room temperature and a strain rate of 10 s^{-1} are listed in Table 3 and used for the springback evaluation. The true stress vs. plastic strain is calculated using the stress–strain relationship from Ref. [27] and is shown in Figure 1. Polypropylene is modelled using a piecewise linear plasticity model, Mat_24 in LS-DYNA.

Table 3. Mechanical properties of polypropylene.

Property	Value	Units
Density	900	kg/m ³
Modulus of elasticity	2.443	GPa
Yield Strength	25	MPa
Poisson’s ratio	0.43	-

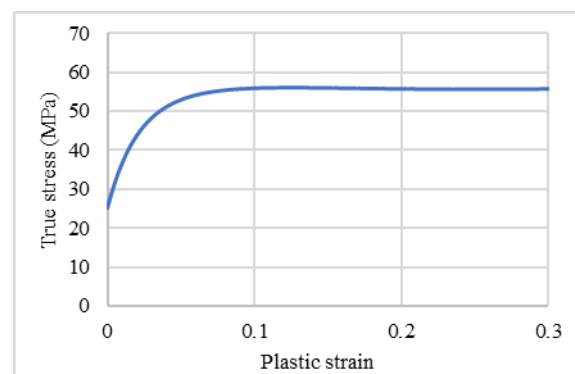


Figure 1. Plastic stress–strain curve of polypropylene at room temperature and strain rate of 10^{-1} s .

2.1. Finite Element Model

Springback of single SA5182 aluminum sheets is studied using the draw-bend setup for forming U-channels defined in Numisheet’93 [28]. A quarter model is built in LS-DYNA applying symmetry conditions to reduce computation time. The model consists of a rigid die, punch, blank holder and a deformable blank similar to Figure 2a. The blank size has the aerial dimensions of $320 \text{ mm} \times 35 \text{ mm}$. A blank length of 320 mm is used instead of 350 mm to match the blank length used in the springback experiments described later. A total blank holder force of 2500 N is applied. The blank is drawn to a depth of 70 mm with a punch velocity of 200 mm/sec . The tools and the blank are modelled using fully integrated 4-noded quadrilateral shell element formulation (type 16 in LS-DYNA) recommended for springback simulations by Maker and Zhu [29]. To understand the bending and springback behavior of monolithic aluminum sheets in draw-bending simulations, nine integration points through the sheet thickness are used in this study. Springback is characterized by measuring the change in shape along the side wall and the flange. The angular changes

in the sidewall and the flange are measured by the wall angle θ_1 and the flange angle θ_2 , respectively. The description of θ_1 and θ_2 along with the standard procedure given in Numisheet'93 is followed to make these measurements uniform as shown in Figure 2b. In addition to the wall and flange angles, the curvature of the wall of the formed U-channel, referred to as the sidewall curl, is measured by its radius ρ . The radius of curvature is measured by the radius of a curve fitted through three points A, B and C as shown in Figure 2b. Here, C is the midpoint between A and B. In this study, the springback angles θ_1 and θ_2 are measured in CATIA V5 using the meshes at the end of the springback simulation obtained from LS-DYNA.

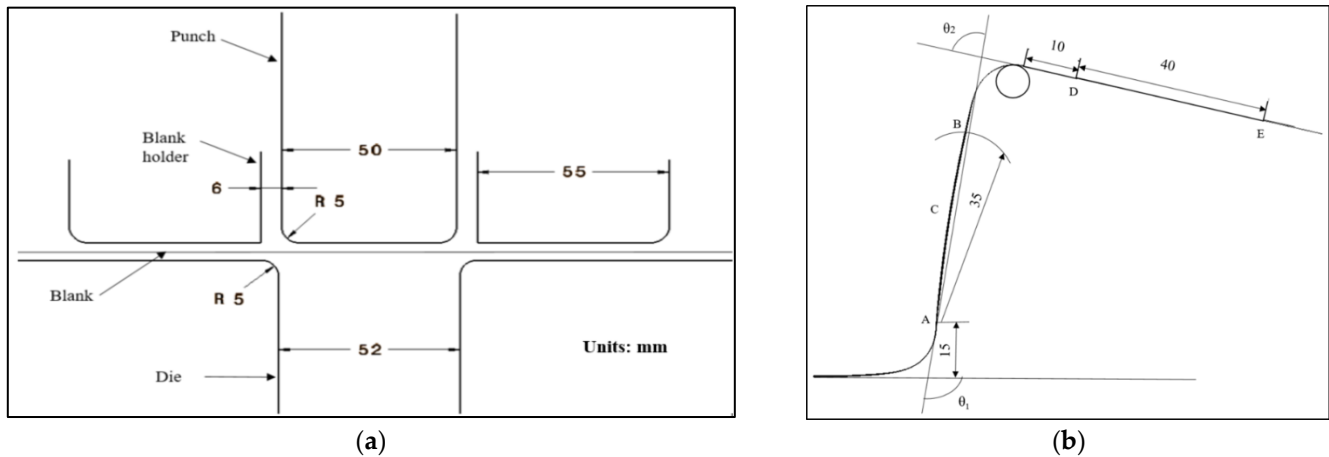


Figure 2. (a) Dimensions of the draw-bend setup for forming a U-channel according to Numisheet'93 (b) Springback measurements for a drawn U-channel according to Numisheet'93.

2.2. Finite Element Model for Sandwich Laminates

The springback of SA5182/polypropylene/SA5182 laminates is assessed by using the same setup as described in Section 2.1. The aerial dimensions of the blank are 320 mm \times 35 mm. The laminate thickness is in the range of 1.2 to 2.6 mm and is made of various combinations of core and skin thicknesses. The aluminum skin thicknesses are 0.2, 0.22, 0.24 and 0.25 mm. The polypropylene core thicknesses are 0.8, 1.0, 1.6, 1.9 and 2.2 mm. U-channel draw-bending experiments conducted with 0.2/0.8/0.2 mm sandwich laminates in a die-punch setup with 5 mm die-punch radii have shown early cracking at the punch corners at a draw depth of approximately 8 mm. Therefore, to study the springback behavior of the sandwich laminates, the die and punch radii are both increased to 8 mm.

The aluminum/polypropylene/aluminum sandwich blank is modeled with Part_Composite shell elements available in LS-DYNA. Unlike the traditional method that requires a separate mesh for each material, Part_Composite allows the use of a single shell mesh within which individual layers of the sandwich laminate are defined by their thickness and integration points. The integration points are located at the center of each layer thickness. Thus, the aluminum skins are defined by three integration points each and the polypropylene layer is defined by four integration points. The Part_Composite elements use trapezoidal integration rule. Adaptive mesh is used in the model with up to four levels of refinement to capture the die and punch radii more accurately.

3. Results and Discussions

3.1. Springback of Single SA5182 Sheets

The effect of sheet thickness on the springback of SA5182 is studied by considering a thickness range of 0.2 mm to 1.2 mm in steps of 0.2 mm. The blank size has the aerial dimensions of 320 mm \times 35 mm. The punch diameter is 50 mm, and the die-punch gap is adjusted based on the sheet thickness so that there is no ironing as the U-channel is formed.

The results presented in Figure 3 show that as the sheet thickness increases from 0.2 mm to 1.2 mm, the springback of the SA5182 aluminum sheets shows a stiffer response,

meaning that the wall angle reduces, while the flange angle increases with increasing sheet thickness. The radius of curvature controlling the sidewall curl also increases when the sheet thickness increases. The U-channel profiles after springback are shown in Figure 4.

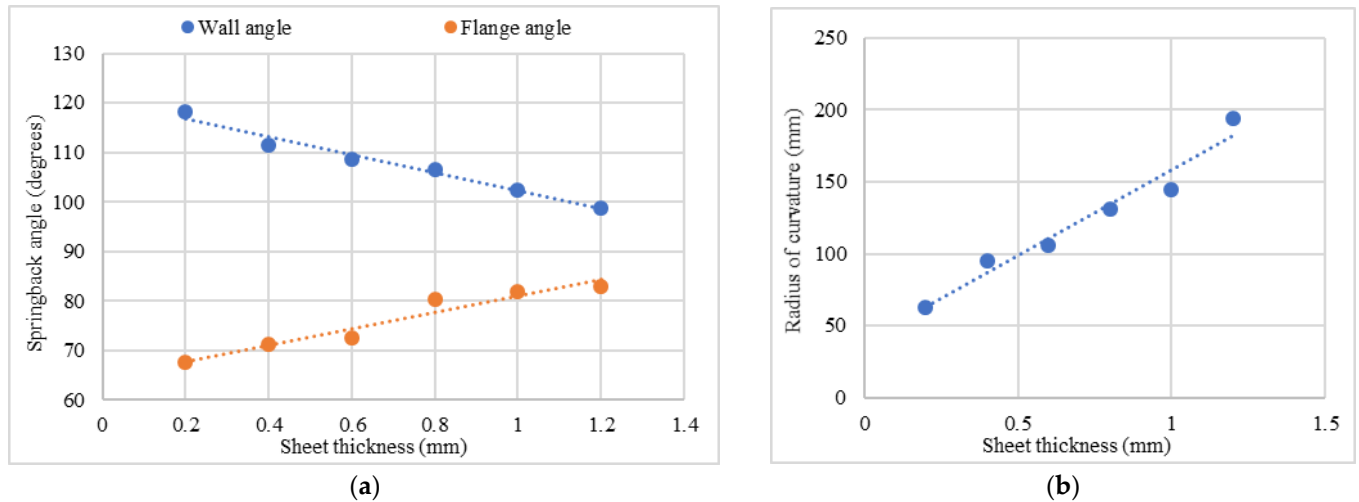


Figure 3. (a) Effect of sheet thickness on the springback angles of SA5182 and (b) Variation of radius of curvature of the wall with sheet thickness for SA5182.

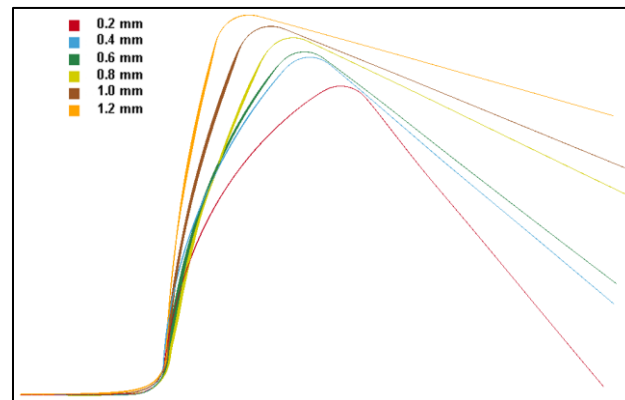


Figure 4. Springback profiles of single SA5182 U-channels with sheet thickness ranging from 0.2 mm to 1.2 mm.

Since springback after U-channel forming involves bending deflection of its walls and flanges, the effect of the sheet bending stiffness on the springback angles, and the radius of curvature is considered. The bending stiffness of single aluminum sheets is calculated using Equations (1) and (2).

$$\text{Bending stiffness} \propto EI \tag{1}$$

$$\text{Second moment of area } I = bt^3/12 \tag{2}$$

where b is the width of the sheet, which for the U-channels is 35 mm, and t is the thickness of the sheet.

The springback angles are plotted against the bending stiffness of the SA5182 sheets with different thicknesses in Figure 5a. It can be seen in this figure that the wall angle decreases, and the flange angle increases with increasing bending stiffness until it reaches a value of 200,000 N-mm². At higher bending stiffnesses, the springback angles do not show much variation. However, as can be seen in Figure 5b, the radius of curvature of the wall increases with increasing bending stiffness, indicating that there is less wall curl, even at bending stiffnesses higher than 200,000 N-mm².

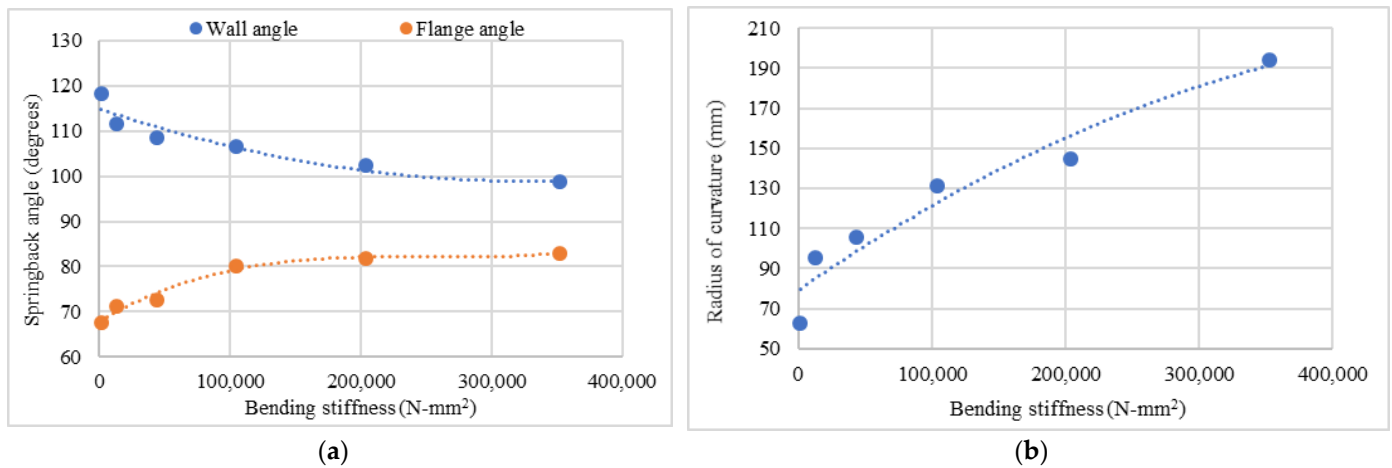


Figure 5. (a) Wall angle and flange angle vs. bending stiffness of single SA5182 sheets and (b) Variation of radius of curvature of the wall of SA5182 sheets with bending stiffness.

Table 4 shows the springback values of SA5182 U-channels for two different die/punch radii, 5 mm and 8 mm. Comparing the two sets of springback values, it can be observed that overall, springback for single SA5182 is reduced with an increase in die/punch radii from 5 mm to 8 mm. While the improvements in wall and flange angles are relatively small, there is a large increase in the radius of curvature of the wall. This means that the side wall curl is reduced significantly as the radii of the die and punch are increased.

Table 4. Springback values for single SA5182 with die/punch radii of 5 mm and 8 mm.

Sheet Thickness (mm)	Die and Punch Radii = 5 mm			Die and Punch Radii = 8 mm		
	θ_1 (°)	θ_2 (°)	ρ (mm)	θ_1 (°)	θ_2 (°)	ρ (mm)
0.8	106.58	80.22	131.12	102.10	84.50	246.54
1	102.29	81.87	145.00	101.68	84.71	259.64
1.2	98.64	83.02	194.21	98.89	85.27	290.17

3.2. Springback of SA5182/Polypropylene/SA5182 Sandwich Laminates

3.2.1. Effect of Laminate Thickness

The measurements of θ_1 , θ_2 and ρ for the U-channels after springback are made as described in Section 2.1. The springback values obtained for different thickness combinations of aluminum skins and polypropylene core for the 8 mm die/punch radii are shown in Figure 6. The wall angle θ_1 is directly influenced by the total thickness of the sandwich laminate, while the flange angle θ_2 is additionally dependent on the sidewall curl in the U-channel. A large value of radius of curvature indicates reduced sidewall curl.

From Figure 6a it can be seen that the wall angle θ_1 decreases with increasing laminate thickness and the flange angle θ_2 shows an increasing trend with increasing laminate thickness. However, as the laminate thickness becomes higher than 2.5 mm, changes in both wall and flange angles become relatively small. In Figure 6b, the radius of curvature of the wall is plotted against the laminate thickness. There is an increase in the radius of curvature, and therefore a decrease in sidewall curl up to a laminate thickness of about 2 mm after which it shows a reverse trend.

The springback variation of Al/PP/Al laminates cannot be explained solely as a function of laminate thickness, since it is also dependant on the volume fraction of each component material and the overall stiffness of the sandwich laminate. Therefore, further comparisons are made to study the springback behavior with laminate stiffness. For a given symmetric 3-layered sandwich laminate of skin thickness (t) and core thickness (d), the bending stiffness EI is calculated using Equation (3) taken from ref. [30].

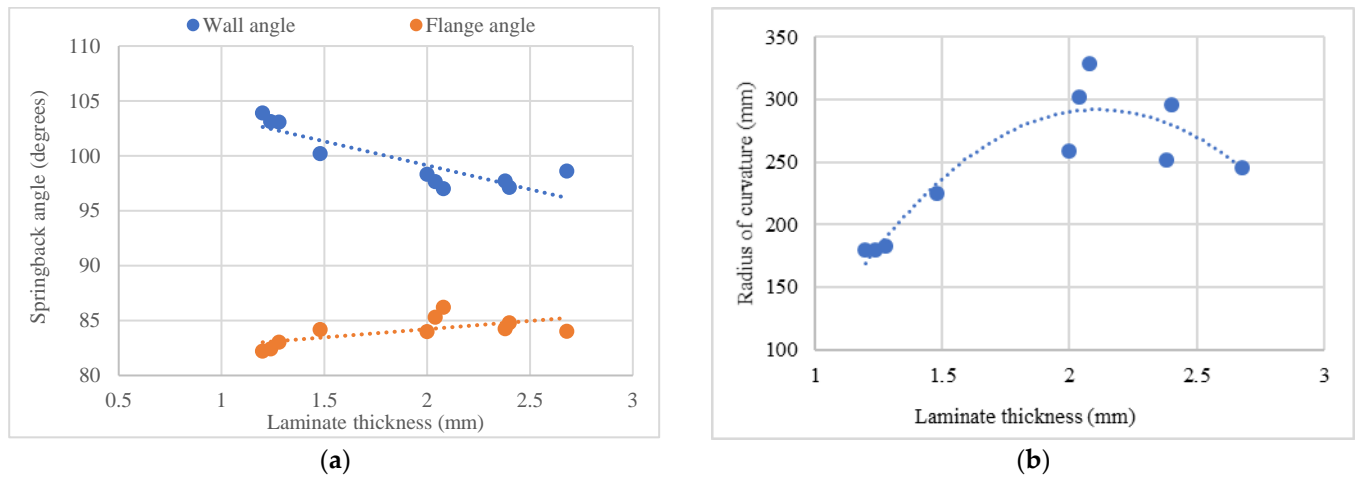


Figure 6. (a) Variation of wall and flange angles with laminate thickness (b) Variation of radius of curvature of the wall with laminate thickness.

$$EI_{Laminate} = E_s \left(\frac{bt^3}{6} \right) + 2bE_s t \left\{ \frac{d+t}{2} \right\}^2 + E_c \left(\frac{bd^3}{12} \right) \quad (3)$$

The bending stiffness calculated for each thickness combination is listed in Table 5. The graph plotted between wall angle and bending stiffness in Figure 7a shows that wall angle decreases with increasing bending stiffness up to a laminate stiffness of $11.5 \times 10^6 \text{ N}\cdot\text{mm}^2$ and then starts to show an increase. In comparing the wall angles of the single aluminum sheet and the Al/PP/Al laminate with the same bending stiffness, it can be seen that the laminate shows a greater springback. Similarly, the flange angles for the Al/PP/Al laminates plotted against the bending stiffness in Figure 7b are lower than the flange angles of the single aluminum sheets for the same bending stiffness. It can be seen that flange angle increases with bending stiffness, reaches a maximum and then decreases. The radius of curvature of the wall also increases with increasing bending stiffness up to a laminate stiffness of $11.5 \times 10^6 \text{ N}\cdot\text{mm}^2$ and then decreases (Figure 8). These results show that single aluminum sheets with equal bending stiffness as Al/PP/Al laminates have better springback performance.

Table 5. Bending stiffness and springback of SA5182/Polypropylene/SA5182 laminates.

Skin Thickness, t (mm)	Core Thickness, d (mm)	Laminate Stiffness (N·mm ²)	θ ₁ (°)	θ ₂ (°)	ρ (mm)
0.20	0.8	251,914.88	103.90	82.21	179.58
0.22	0.8	288,383.95	103.11	82.42	179.44
0.24	0.8	327,283.41	103.07	83.02	183.12
0.24	1.0	464,824.62	100.19	84.18	224.93
0.20	1.6	826,252.37	98.31	83.98	258.61
0.22	1.6	926,225.44	97.65	85.30	302.00
0.24	1.6	1,030,196.91	97.00	86.20	329.00
0.24	1.9	1,400,920.43	97.71	84.25	251.50
0.25	1.9	1,470,894.07	97.12	84.78	296.12
0.24	2.2	1,831,874.64	98.60	84.02	245.51

In comparing the springback values of single aluminum sheet and the sandwich laminates (Table 6), it can be seen that the 0.2/0.8/0.2 mm laminate has a lower bending stiffness and shows a greater degree of springback compared to the single aluminum sheet of equal thickness. The 2 mm thick sandwich laminate with 0.2/1.6/0.2 mm thickness combination has springback values close to those of the 1.2 mm thick single aluminum sheet. Its bending stiffness is higher than twice the bending stiffness of the single aluminum sheet. Thus, the springback response of sandwich laminates is higher than that of the

single aluminum sheet if they have the same thickness. Equal springback response is obtained when the bending stiffness of the sandwich laminate is higher than that of the single aluminum sheet.

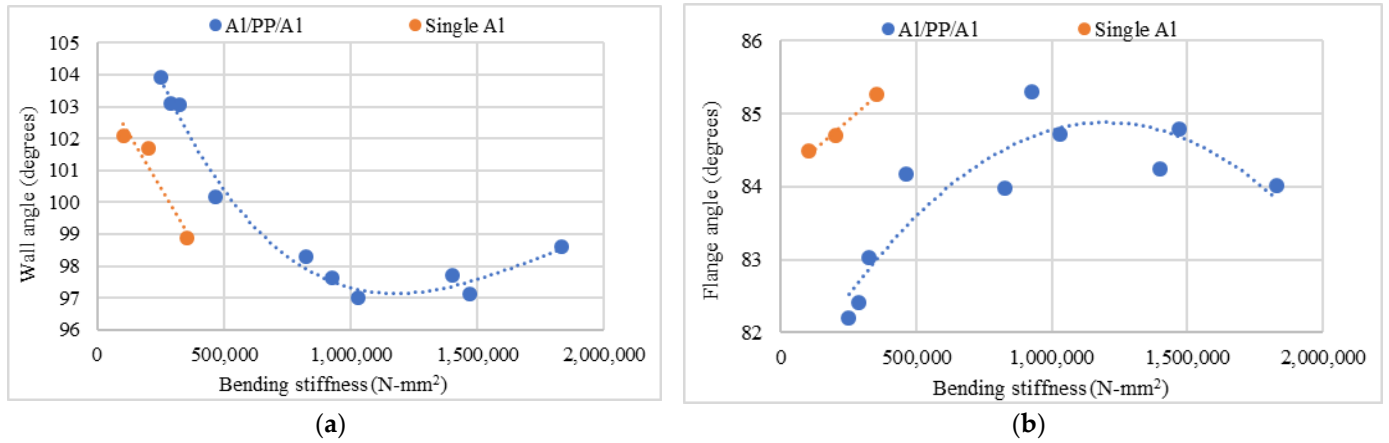


Figure 7. (a) Wall angle vs. bending stiffness of single Al and Al/PP/Al laminates (b) Flange angle vs. bending stiffness of single Al and Al/PP/Al laminates.

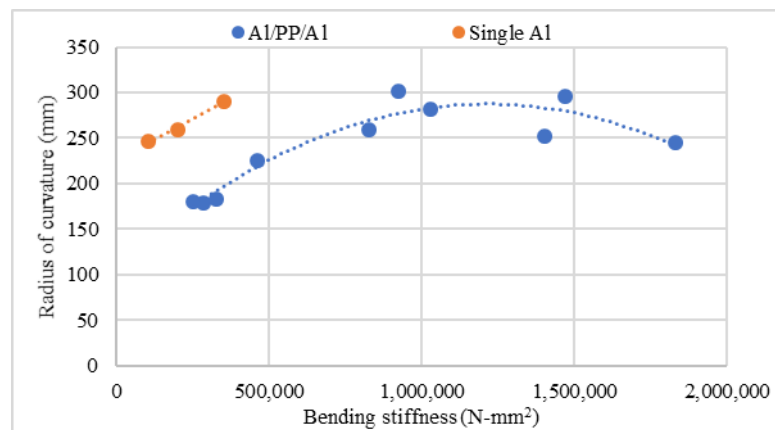


Figure 8. Radius of curvature vs. bending stiffness of single Al and Al/PP/Al laminates.

Table 6. Comparison of springback angles and radius of curvature of U-channels of a single aluminum sheet and two Al/PP/Al sandwich laminates.

	Thickness (mm)	Bending Stiffness (N-mm ²)	θ_1 (°)	θ_2 (°)	ρ (mm)
Single Al	1.2	352,800.00	98.89	85.27	290.17
Al/PP/Al	0.2/0.8/0.2	251,914.88	103.90	82.21	179.58
Al/PP/Al	0.2/1.6/0.2	797,066.67	98.31	83.98	258.61

3.2.2. Effect of Skin and Core Thickness

The effects of the skin and core thickness are individually considered in this section. From Figure 9 it can be seen that at a constant core thickness, the U-channel shows reduced springback behavior in both wall and flange angles with increasing skin thickness. Figure 9a,b also show that the wall angle is significantly lower with 1.6 mm core thickness, while the flange angle is significantly higher with 1.6 mm core thickness, both indicating that springback decreases with increasing core thickness.

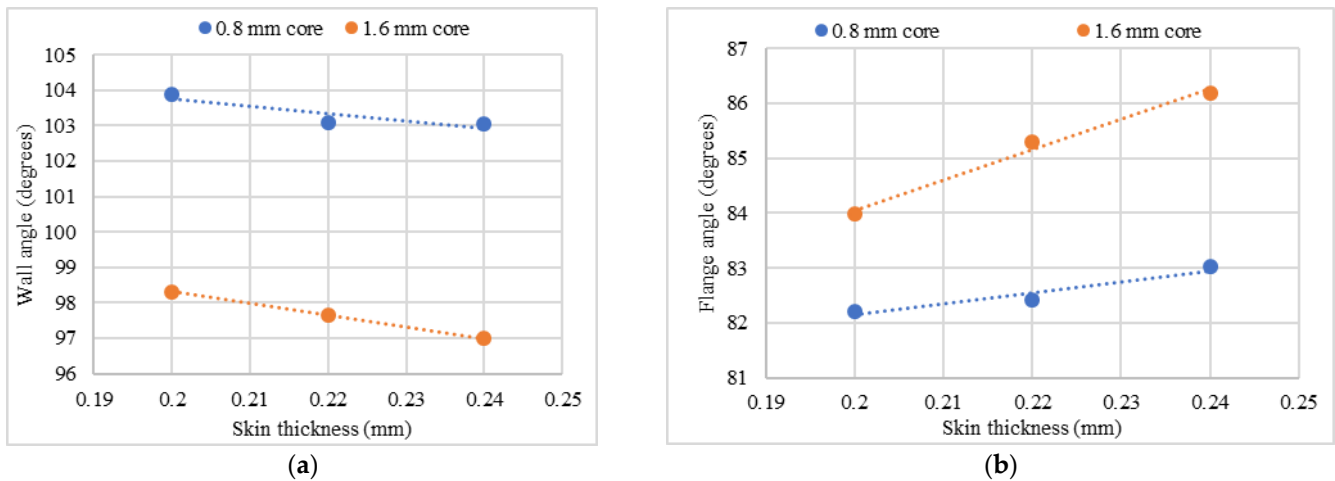


Figure 9. (a) Wall angle and (b) flange angle with varying skin thickness for laminates with 0.8 mm and 1.6 mm core thicknesses.

The beneficial effect of increasing skin thickness can be seen in the shapes of the U-channels (Figure 10) at the end of the springback simulation for 0.2, 0.22 and 0.24 mm skin thicknesses with the core thickness maintained at a constant value of 1.6 mm.

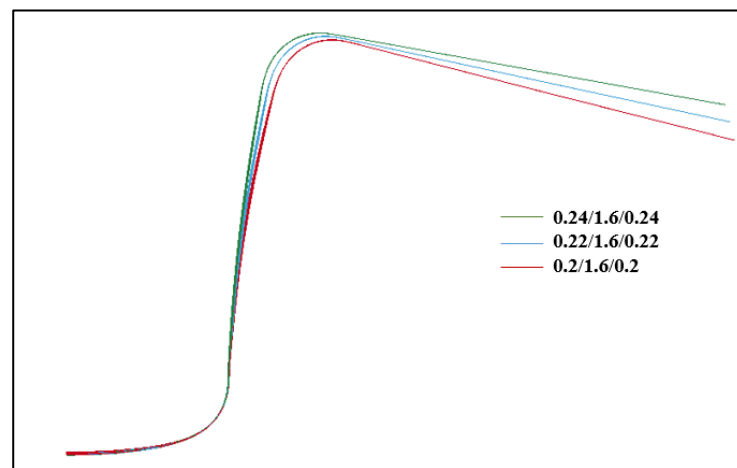


Figure 10. Shapes of U-channels after springback, with 0.2, 0.22, 0.24 mm skin thickness and a constant core thickness of 1.6 mm.

Although increasing the core thickness shows an overall improvement in springback behavior, i.e., the wall angle reduces and the flange angle increases, it is true only up to a certain core thickness. In Figure 11a, the wall and flange angles for constant skin thickness of 0.24 mm are plotted against core thicknesses of 0.8, 1.0, 1.6, 1.9 and 2.2 mm. Increasing the core thickness above a value of 1.6 mm shows an increase in the wall angle and a decrease in the flange angle. Figure 11b shows the U-channels after springback with varying core thicknesses and a constant skin thickness of 0.24 mm.

The change in springback behavior at higher than 1.6 mm core thickness is further investigated and is found to occur due to very high plastic strains in the outer aluminum skins for the thicker sandwich laminates with a core thickness of 1.6 mm and higher. The effective plastic strains (EPS) in each layer of the sandwich laminates with skin thickness of 0.24 mm and varying core thicknesses of 0.8, 1.0, 1.6 and 1.9 mm are plotted in Figure 12. It can be seen that EPS values for the laminates with 0.8 mm and 1.0 mm core thickness are low. The 1.6 mm core sandwich shows high plastic strains in the lower skins, while the 1.9 mm core thickness sandwich shows much higher plastic strains in both upper and lower aluminum skins that have led to excessive thinning in the U-channel walls. Therefore, the

reversing trend in wall and flange angles with core thickness is probably due to high plastic strains in the lower and upper skins of the sandwich laminates with core thickness greater than 1.6 mm.

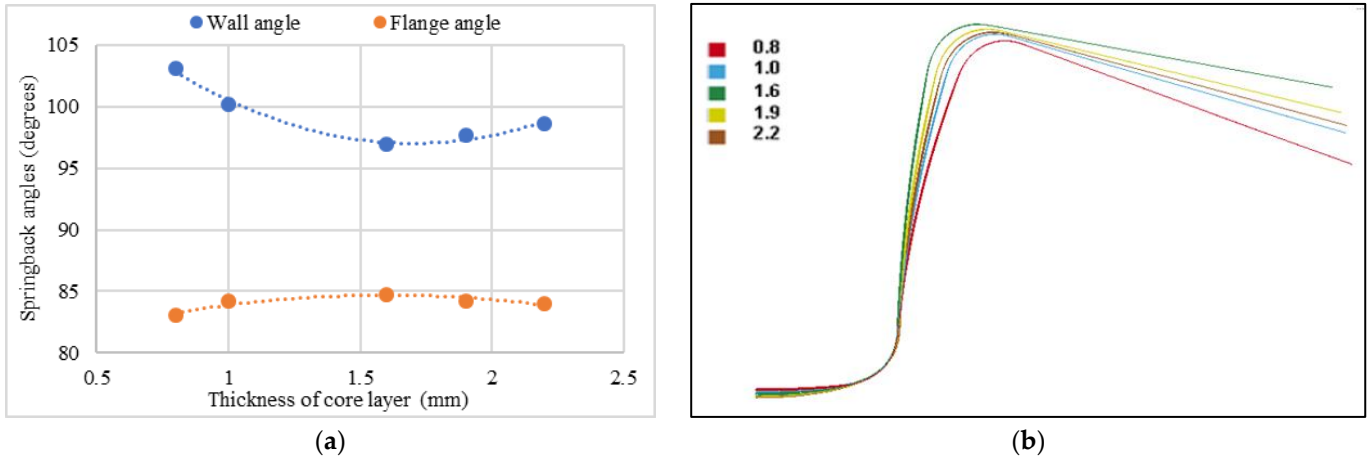


Figure 11. Effect of increasing core thickness at a constant skin thickness of 0.24 mm on (a) springback angles (b) U-channel profiles.

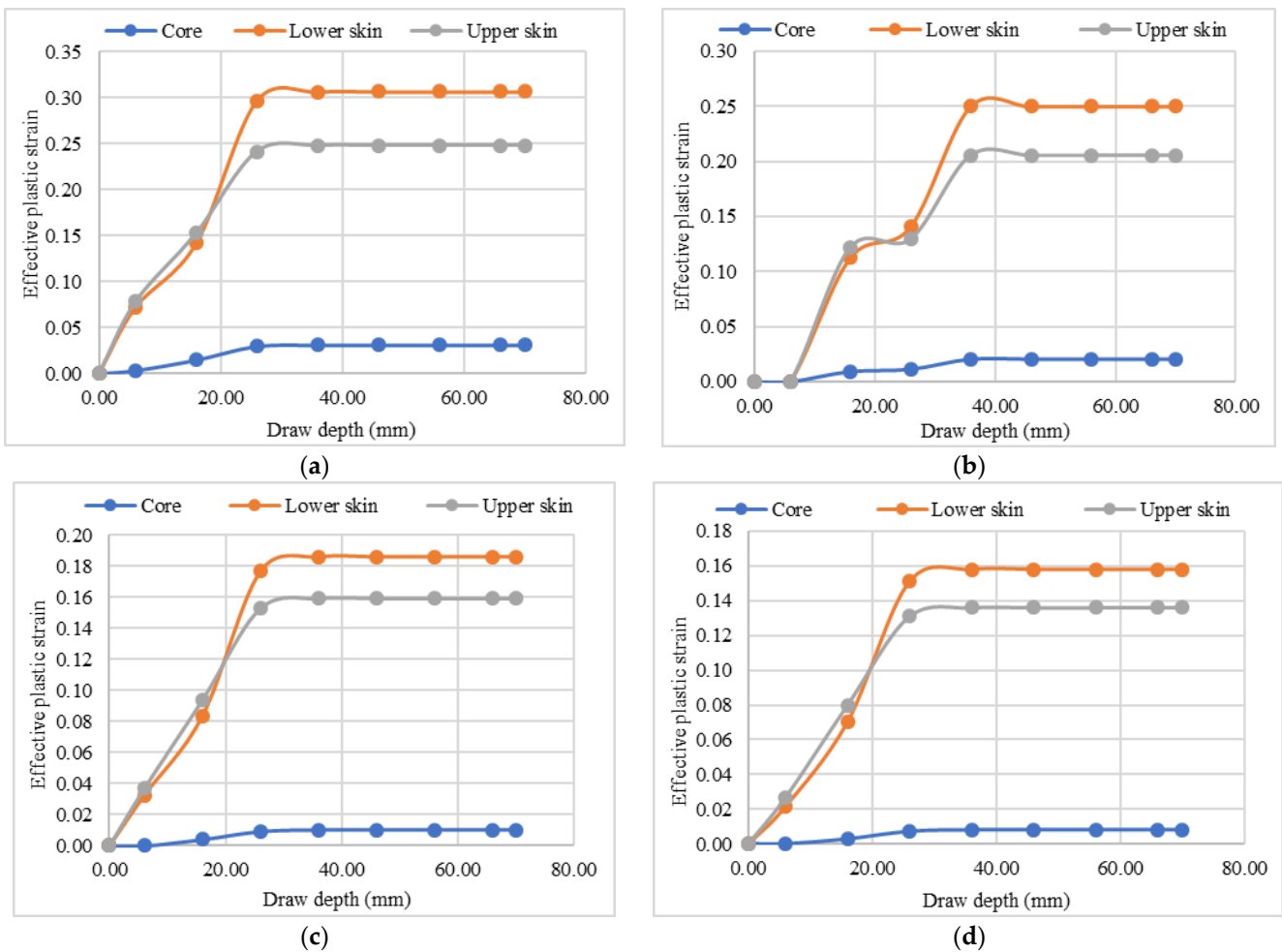


Figure 12. Effective plastic strains in sandwich laminates at the end of 70 mm draw depth. The thickness combinations are (a) 0.24/1.9/0.24 mm (b) 0.24/1.6/0.24 mm (c) 0.24/1.0/0.24 mm (d) 0.24/0.8/0.24 mm.

In addition to the core and skin thicknesses, there are several tool design and process parameters, such as punch and die radii and blank holder force, that have effect on the springback of Al/PP/Al laminates. The effects of such parameters have been studied extensively for monolithic sheet metals, some of which can be seen in refs. [31,32]. The parameters considered in this study, their range and justification are given in Table 7 and their effects are described in Sections 3.2.3–3.2.7.

Table 7. List of tool design and process parameters studied for springback of Al/PP/Al sandwich laminates.

Parameter	Range	Justification of Selected Range
Punch Radius (Die radius = 8 mm, BHF = 2500 N, sidewall clearance = 0.3 mm)	5–12 mm	The punch and die radius range is chosen based on previously published research [31,33]
Die Radius (Punch radius = 8 mm, BHF = 2500 N, sidewall clearance = 0.3 mm)	5–12 mm	
Blank Holder Force (BHF) (punch/die radius = 8 mm, sidewall clearance 0.3 mm)	500–2500 N	Lower range of BHF is used to keep the plastic strains in the aluminum skins below failure strain
Punch-die Gap/Sidewall Clearance (punch/die radius = 8 mm, BHF = 2500 N)	0.1–0.3 mm	Numisheet’93 has 0.2 mm clearance. A 0.1 mm higher and lower clearance was considered

3.2.3. Effect of Punch Radius

First, the variation of punch radius is examined. Punch radii of 5 mm, 8 mm, 10 mm and 12 mm are modelled with a constant die radius of 8 mm in the numerical simulations. All other parameters remain the same. The wall and flange angles for each punch radius are plotted for three different laminate thickness combinations 0.2/0.8/0.2, 0.2/1.6/0.2 and 0.25/1.9/0.25 mm.

In Figure 13a, the wall angle shows an overall increasing trend with increasing punch radius. Changing the punch radius has a more significant effect on the wall angle for sandwich laminates with a core thickness of 0.8 mm. Increasing the punch radius shows an increase in flange angle (Figure 13b) for all three thickness combinations of the sandwich laminate. Here, increasing the punch radius seems to have a greater effect on the flange angles for the laminates with thicker cores (1.6 mm and 1.9 mm).

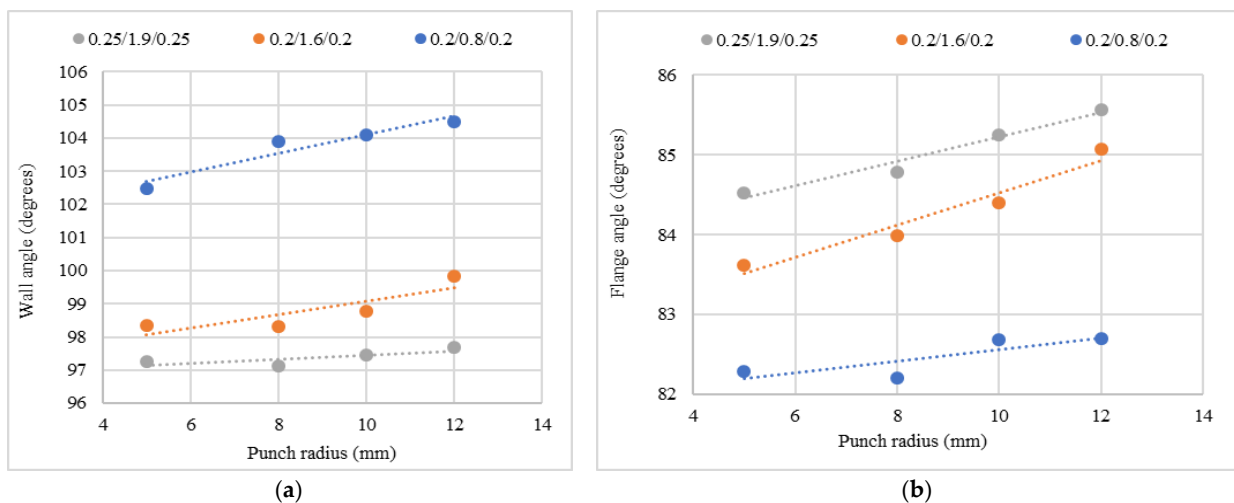


Figure 13. (a) Effect of punch radius on wall angle after springback and (b) Effect of punch radius on flange angle for three different sandwich laminate thickness combinations and a constant die radius of 8 mm.

The radius of curvature shows a slight increase with punch radius for the 0.2/1.6/0.2 mm and 0.25/1.9/0.25 mm laminates but does not vary much for the 0.2/0.8/0.2 mm laminate (Figure 14a). The shapes of the sandwich laminate U-channel for different punch radii at the end of springback are shown in Figure 14b.

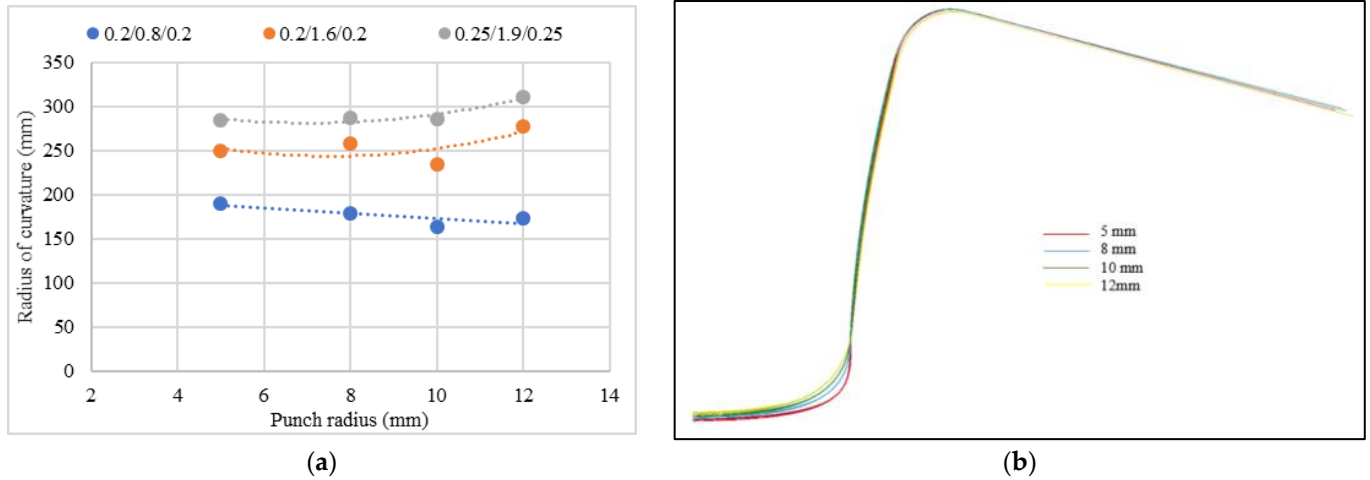


Figure 14. (a) Effect of punch radius on radius of curvature for three different sandwich laminate thickness combinations and constant die radius of 8 mm, and (b) Springback profiles of 0.2/1.6/0.2 mm sandwich laminates with different punch radii and a constant die radius of 8 mm.

3.2.4. Effect of Die Radius

It can be seen from Figure 15a that as the die radius changes from 5 mm to 12 mm, the wall angle decreases. The punch radius is 8 mm in all these cases. More significant decrease is noted in the sandwich laminates with a thicker polypropylene core. It can also be seen that for all sandwich thicknesses, the flange angle increases with increasing die radius as shown in Figure 15b. Another observation is that at die radii of 10 mm and 12 mm, the sandwich laminates with 1.6 mm and 1.9 mm core thicknesses show nearly equal flange angles.

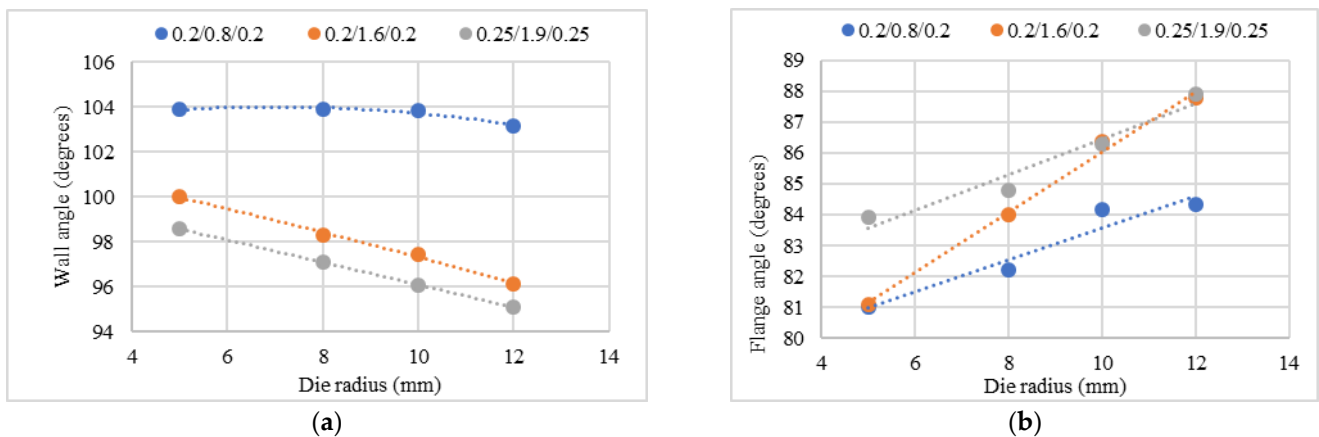


Figure 15. Effect of die radius on (a) wall angle and (b) flange angle after springback for three different sandwich laminate thickness combinations and a constant punch radius of 8 mm.

Similarly, the radius of curvature shows an increase with increasing die radius, indicating a decrease in sidewall curl. This reduction in sidewall curl is more prominent in the 0.2/1.6/0.2 mm and 0.25/1.9/0.25 mm sandwich laminates (Figure 16a) The shapes of the U channel after springback for a laminate with 0.2/1.6/0.2 mm thickness combination is compared for different die radius values in Figure 16b.

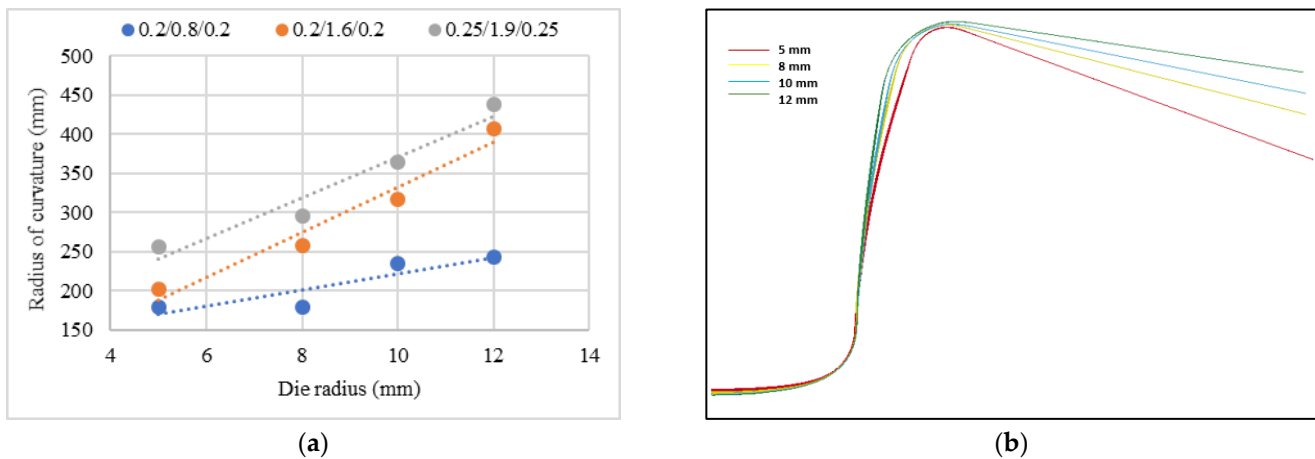


Figure 16. (a) Effect of die radius on radius of curvature after springback for three different sandwich laminate thickness combinations and a punch radius of 8 mm and (b) Springback profiles of 0.2/1.6/0.2 mm sandwich laminates with different die radii and a punch radius of 8.

3.2.5. Effect of Blank Holder Force

A study conducted by Kadkhodayan and Zafarparandeh [34] on the influence of blank holder force (BHF) for DP-steel and AA5754-O shows an initial increase in springback behavior at low BHF followed by a decrease in springback at higher BHF. Another study conducted by Tong and Nguyen [33] on U-draw bending of DP350 shows that wall and flange angles improve up to a BHF of 8 kN and do not show much change at higher BHF. In both cases the punch radius was larger than the die radius and the BHF ranges from 2.5 k to 25 kN. In comparing the springback results of a draw formed and crash formed part by experiment, Stein [32] found that the springback increased when the additional tension was applied using BHF and attributed it to the sidewall curl. The effect of BHF on the springback of Al/PP/Al sandwich laminates is studied in this section using four different blank holder forces, namely 500 N, 900 N, 1700 N and 2500 N. The die and punch radii are 8 mm.

The wall angle increases with increase in blank holder force for all thickness combinations (Figure 17a). The flange angle first decreases and then increases with increasing blank holder force for the sheets with 0.8 mm core. A similar, but much smaller effect is seen with the 1.6 mm and 1.9 mm core thicknesses. Figure 18a shows the reduction in radius of curvature as the blank holder force increases. For a thickness combinations of 0.2/0.8/0.2 and 0.24/0.8/0.24 mm, the radius of curvature is almost unaffected by the blank holder force. Considering the effect of BHF on all three springback parameters, it can be concluded that BHF lower than 2500 N has a negative effect on the springback behavior of the SA5182/PP/SA5182 laminates. Blank holder forces at a higher range may be investigated to see if further increase in axial force during draw bending shows any improvement in springback of aluminum/polypropylene/aluminum sandwich laminates.

The load–displacement curves at increasing blank holder forces are plotted in Figure 18b. For a thickness combination of 0.24/0.8/0.24 mm, as the blank holder force increases the punch load increases. A similar relationship between punch load and blank holder force is seen for all sandwich laminate thicknesses. The figure depicts the punch load only for a quarter model. The total punch load to draw the U-channel is four times the predicted punch load from the FE model.

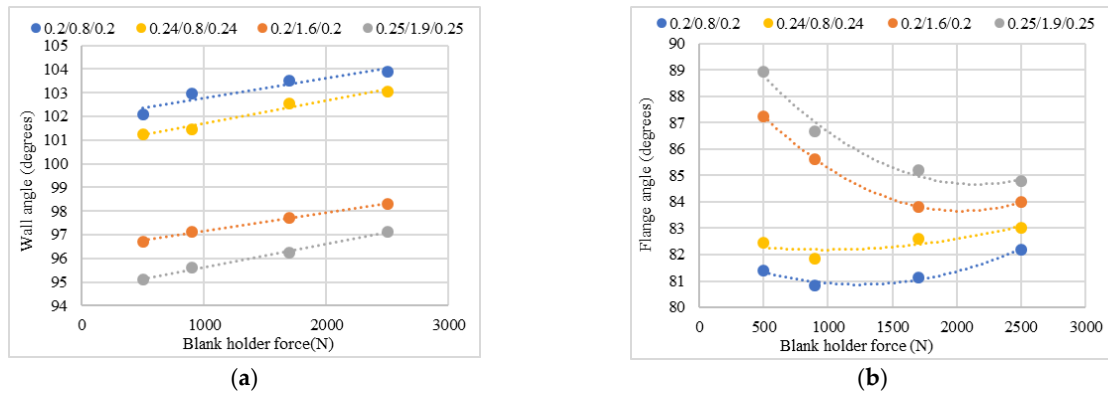


Figure 17. (a) Effect of BHF on wall angle (b) Effect of BHF on flange angle for various thickness combinations of sandwich laminates.

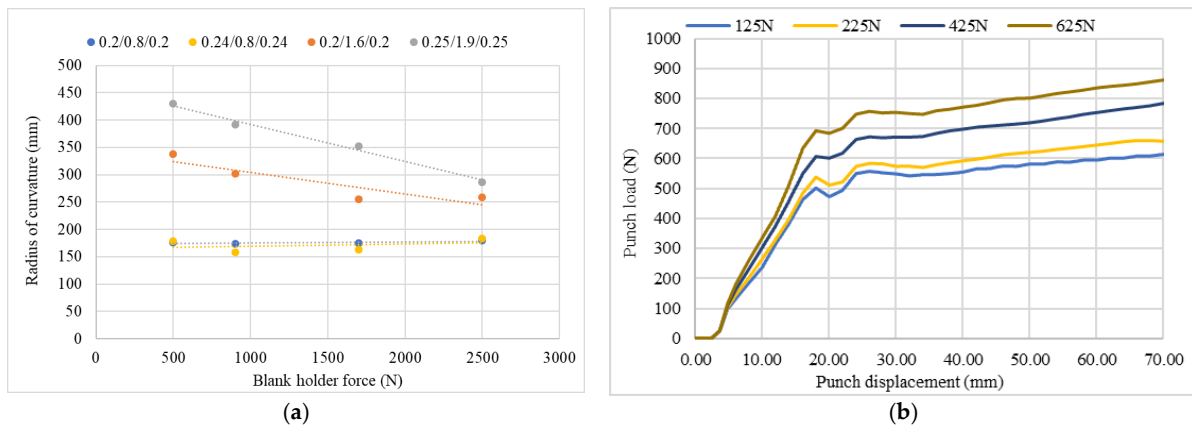


Figure 18. (a) Effect of BHF on radius of curvature (b) Load–displacement curves for varying blank holder force for the sandwich laminate with 0.24/0.8/0.24 mm thickness combination (the BHF’s shown in the legend are for the quarter model).

3.2.6. Effect of Punch-Die Gap

Die-punch gap has proven to be an important parameter in sheet metal forming processes. In the current study, the gap between the punch wall and the die wall is adjusted such that there is no ironing; then for three different thickness combinations, an additional clearance of 0.1 mm to 0.3 mm is added. The difference between die-punch gap and sidewall clearance is shown in Figure 19. Since the die-punch gap is different for each laminate thickness combination, the behavior of wall and flange angles is represented in terms of sidewall clearance in Figure 20.

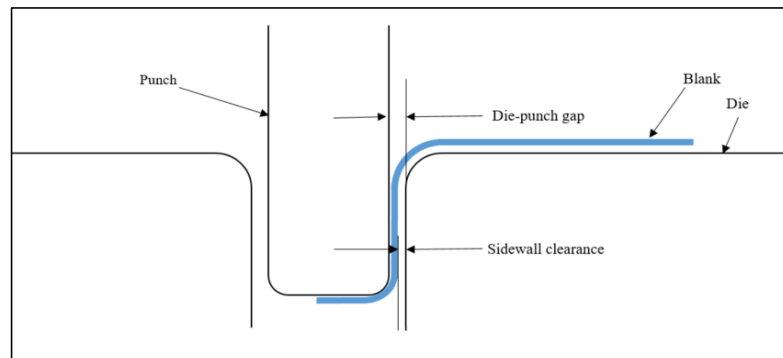


Figure 19. Representation of die-punch gap and sidewall clearance.

The wall angle increases as the sidewall clearance increases for the sandwich laminates with lower core thickness (0.8 mm). For the sandwich laminates of thickness combinations 0.2/1.6/0.2 mm and 0.25/1.9/0.25 mm, the change in wall angle is insignificant. The flange angle decreases with increasing sidewall clearance, i.e., as the gap increases the flange exhibits a more flexible behavior for the sandwich laminates with a core of 0.8 mm and 1.6 mm. The sandwich laminate with 1.9 mm core thickness shows a slightly increasing trend in flange angle with changing punch-die clearance.

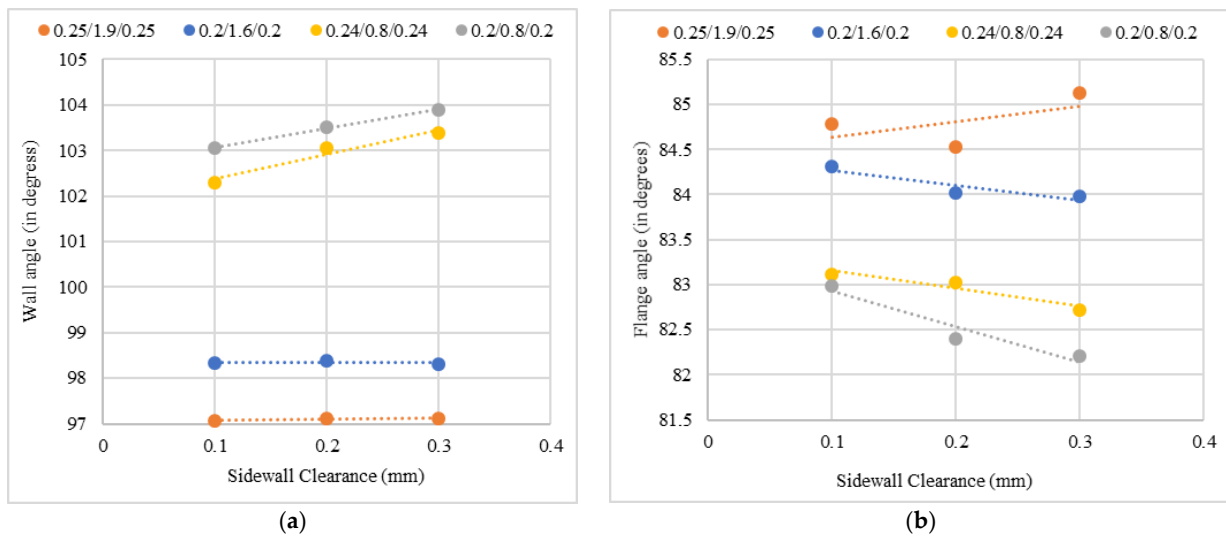


Figure 20. (a) Effect of sidewall clearance on wall angle and (b) flange angle for different thickness combinations of the sandwich laminates.

The variation of radius of curvature with sidewall clearance (Figure 21a) is very similar to the behavior of flange angle. The radius of curvature decreases with increasing sidewall clearance. However, for the 0.25/1.9/0.25 mm laminate, the radius of curvature of the wall remains almost the same when the sidewall clearance is increased from 0.1 mm to 0.2 mm and increases at 0.3 mm. Visually not much difference can be observed between the U-channel profiles after springback for the 0.2/1.6/0.2 mm laminate shown in Figure 21b for different sidewall clearance values, since the wall and flange angles are very close.

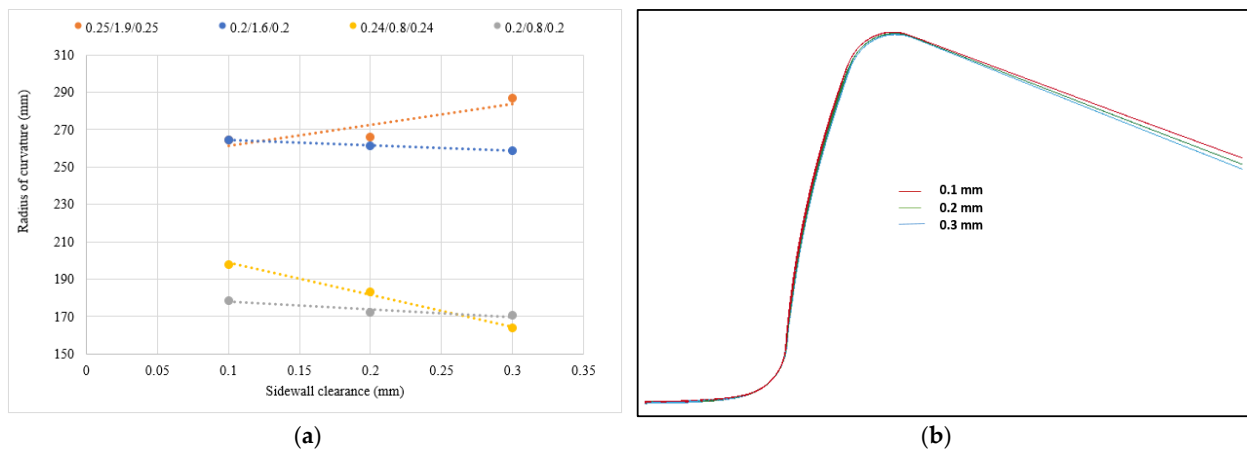


Figure 21. (a) Effect of sidewall clearance on radius of curvature and (b) U-channel profiles after springback for punch-die clearance of 0.1, 0.2 and 0.3 mm for a laminate with a thickness combination of 0.24/0.8/0.24 mm.

3.2.7. Effect of Modelling Approach

Two finite element modelling approaches are compared in this section. The first approach uses the Part_Composite model, which is explained in Section 2.2. The second approach uses a shell-solid-shell model in which the outer aluminum skins are represented by shell elements while the inner polymer core is modelled by solid elements. In this model, the polymer core is tied to the outer skins using tied nodes contact in LS-DYNA to simulate perfect bonding between the core and skin layers of the sandwich laminate. In the shell-solid-shell approach, the aluminum skins are modelled using fully integrated shell element formulation based on Reissner-Mindlin shell model. The polypropylene core is modelled using type-2 fully integrated solid elements. The polymer is modelled using piecewise linear plasticity model (Mat_24) and the aluminum skins are modelled using Yoshida-Uemori hardening model including transverse anisotropy (Mat_125). The finite element mesh for the shell-solid-shell model of the sandwich laminate is shown in Figure 22a.

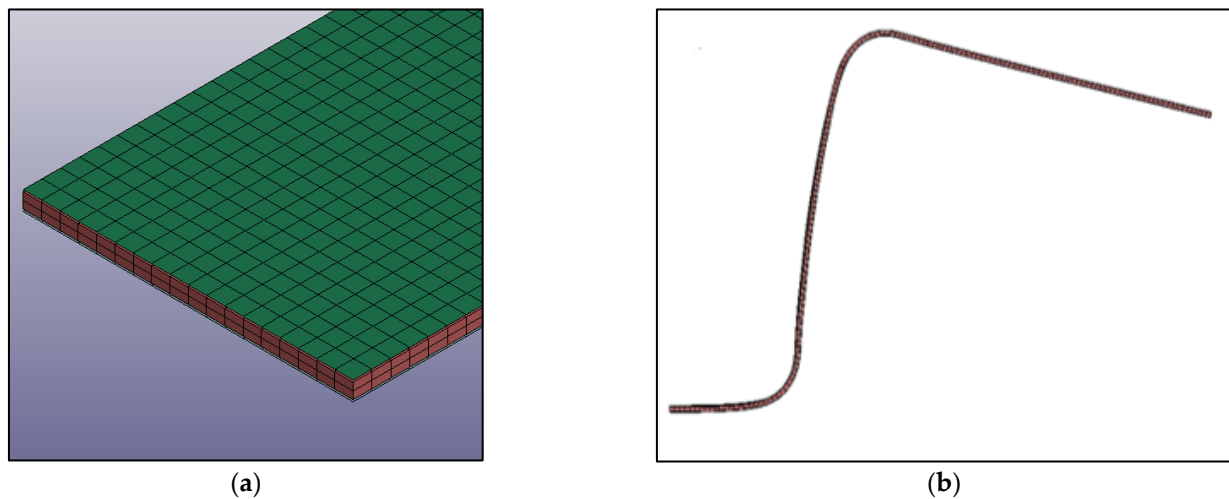


Figure 22. (a) Finite element model with shell-solid-shell elements for the skin-core-skin and (b) Shape of sandwich laminate after springback.

Springback is measured for different thickness combinations of the aluminum skin and polypropylene core. The sandwich laminates with a core thickness of 0.8 mm are modelled with two layers of solid elements through the thickness, resulting in four integration points through the thickness, while those with 1.6 mm core thickness are modelled using four layers of solid elements through the thickness. Three integration points are used for the shell elements that represent the skin.

To evaluate springback in the finite element model, the implicit solver in LS-DYNA is used. The formed U-channel at the end of the explicit forming simulation with element stresses and strains is used as an input for the static implicit analysis. Automatic time step control is invoked and the U-channel is constrained at the node on the plane of symmetry as recommended for LS-DYNA springback inputs by Maker and Zhu [29] to prevent rigid body translations and rotations. The sprung shape of one sandwich laminate (0.2/0.8/0.2) is shown in Figure 22b.

Using the same model parameters as in Section 2.1 with a die/punch radius of 5 mm, a comparison between the two modelling approaches is made in Figure 23. It can be observed in this table that the Part_Composite model mostly shows more conservative values for wall angles. The flange angles show no specific trend between the models. However, the radius of curvature values are very close in both modelling approaches. Overall, the springback angles determined using the two models are in close agreement with each other.

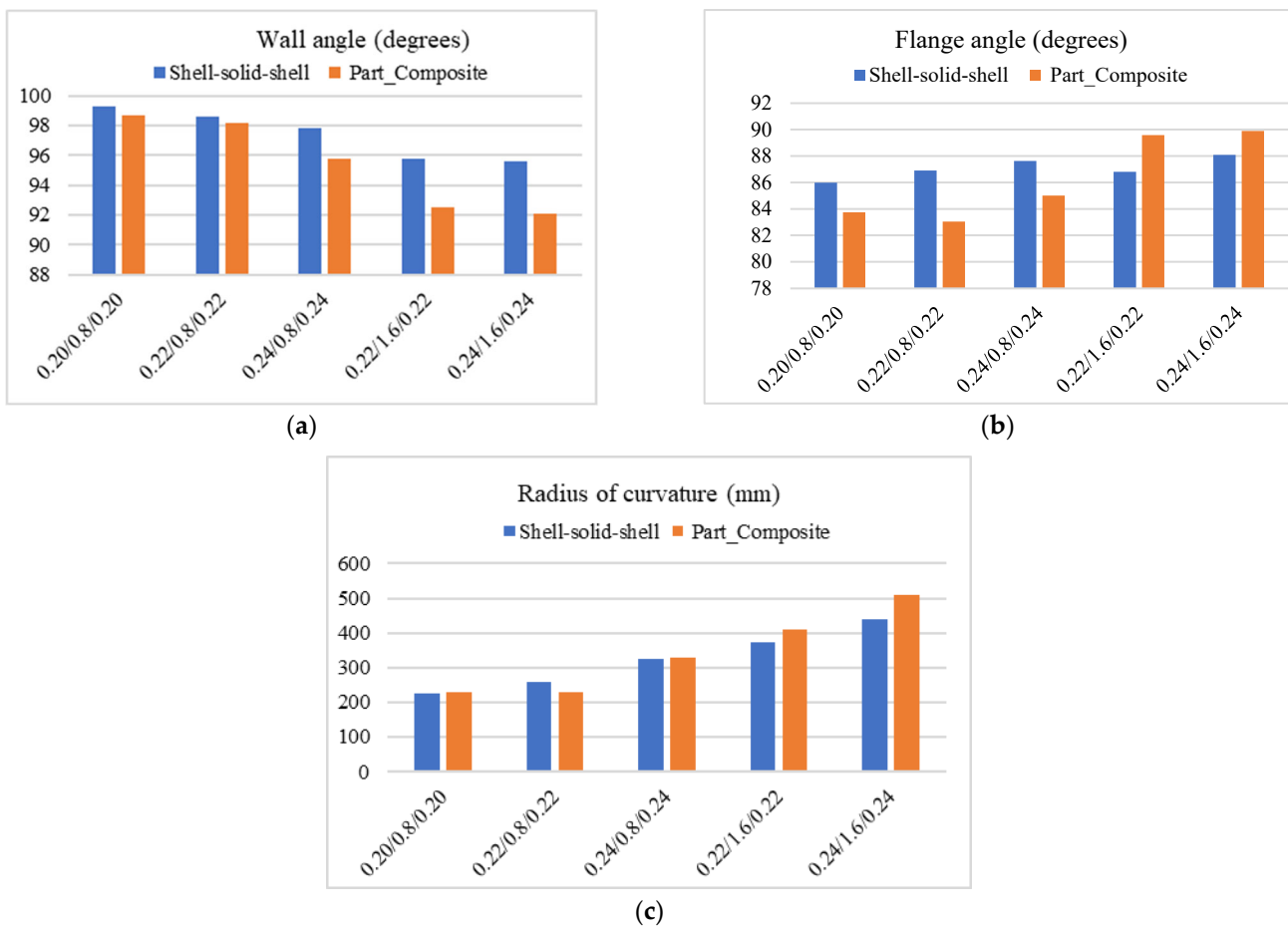


Figure 23. Comparison of springback with different modelling approach (shell-solid-shell and Part_Composite) for a 5 mm die/punch radius (a) Wall angle (b) Flange angle (c) Radius of curvature.

Additionally, a comparison of the wall and flange angles of the 0.20/0.8/0.20 mm sandwich laminate and with 8 mm die/punch radii obtained by the two modelling approaches is made to the experimental values in Table 8. The Part_Composite model shows values closer to the experiment. A clear explanation of the experimental procedure is given in Section 3.2.8. The wall angle predicted by the Part_Composite model is closer to the experiment while both models show nearly the same deviation in flange angle from the experiment. The Part_Composite shows a lower flange angle, while the shell-solid-shell model shows a higher flange angle.

Table 8. Comparison of wall and flange angle for different modelling approach to experiment with 0.20/0.8/0.20 thickness combination and 8 mm die/punch radii.

	Wall Angle (°)	Flange Angle (°)
Shell-solid-shell	99.414	87.049
Part_Composite	103.121	82.946
Experiment (See Section 3.2.8)	104.5	85.0

The CPU time for processing shell-solid-shell model is higher than the Part_Composite model (Table 9). Due to the close agreement of the model’s prediction to the experimental work along with its ease of model set up and lower run time, the Part_Composite model is recommended.

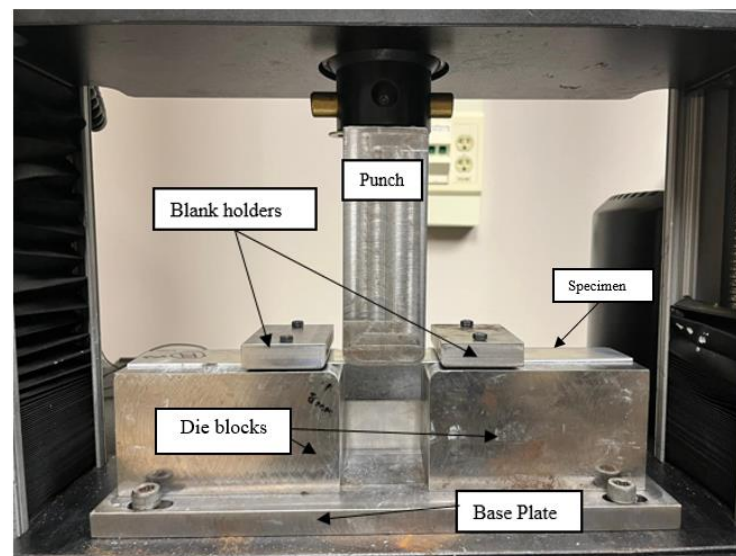
Table 9. CPU processing time for three sandwich thickness combinations with two different modelling approaches.

Al/PP/Al Thickness Combination (mm)	CPU Processing Time (Seconds)	
	Shell-Solid-Shell	Part_Composite
0.20/0.8/0.20	6352	3084
0.22/1.6/0.22	7398	5520
0.24/1.6/0.24	7509	5650

3.2.8. Experimental Work

The experimental set up to determine the springback behavior of SA5182/polypropylene/SA5182 sandwich laminates under draw-bending conditions is based on Numisheet 93 [28] recommendations. In a few initial experiments, the die and punch corner radii were 5 mm; however, since the sheet specimens in these experiments failed by crack formation at the punch corner within 10 mm of punch displacement, it was decided to increase both radii to 8 mm. The simulation studies on the springback of the sandwich laminate reported in the previous sections are also done with 8 mm die and punch radii.

The draw bending tool (Figure 24) consists of a rectangular steel punch attached to the moving crosshead (upper) and two steel die blocks attached to the fixed baseplate on an INSTRON 4469 testing machine. It is designed such that the die-punch gap can be adjusted to accommodate different sheet thicknesses. The blank holder force on each side of the sheet specimen is applied by tightening the bolts connecting the blank holder plates and the die blocks. A digital torque wrench is used to generate the tightening torque needed for the blank holder force (BHF) used for each experiment.

**Figure 24.** Experimental draw bending tool setup installed on an Instron testing machine.

The experiments are carried out for three different thickness combinations. The punch-die gap is adjusted to match the numerical simulations. The punch displacement is controlled by moving the crosshead at 10 mm/min and is made to stop when it reaches 70 mm. The number of tests conducted was one per condition. A metal-to-metal working lubricant (White Lithium) is applied on all contact surfaces. The draw-bended sheet when removed from the fixture springs back freely. The springback angles are calculated by tracing the final shape of the specimen on a blank sheet of paper and making the measurements following the prescribed method in Numisheet 93 [28]. Table 10 lists the springback angles measured from experiments.

Table 10. Experimental springback results for SA5182/Polypropylene/SA5182.

Skin/Core/Skin Thickness Combination	Torque (N-m)	BHF (N)	Wall Angle (θ_1) (°)		Flange Angle (θ_2) (°)	
			Experiment	Simulation ^(a)	Experiment	Simulation ^(a)
0.2/0.8/0.2	0.46	2500	104.50	103.90	85.00	82.20
0.2/0.8/0.2	0.36	1700	102.50	103.49	85.00	81.13
0.2/0.8/0.2	Finger tightened	-	101.20	-	84.50	-
0.22/0.8/0.22	0.46	2500	102.50	103.11	85.00	82.42
0.22/0.8/0.22	0.36	1700	101.50	-	84.50	-

^(a) Part_Composite Model.

The laminate specimens with 0.2/0.8/0.2 and 0.22/0.8/0.22 mm thickness combinations are drawn to 70 mm depth without failure at both 1700 N and 2500 N blank holder forces. In experiments with laminate specimens with 0.2/1.6/0.2 mm combination, failure by cracking occurs at the punch corners at the start of the blank being drawn into the wall of the cup. As the drawing progresses failure is seen at the die corner also. This failure is only in the aluminum skins and does not propagate through the entire thickness of the sheet. It can be observed in Figure 25 and also in Table 10 that as the blank holder force increases, the wall angle increases indicating increase in springback; this is also shown by simulation in Section 3.2.5. The aluminum laminates with 0.2/0.8/0.2 and 0.22/0.8/0.22 mm thickness combinations show springback values in close agreement with the current numerical model in this study.

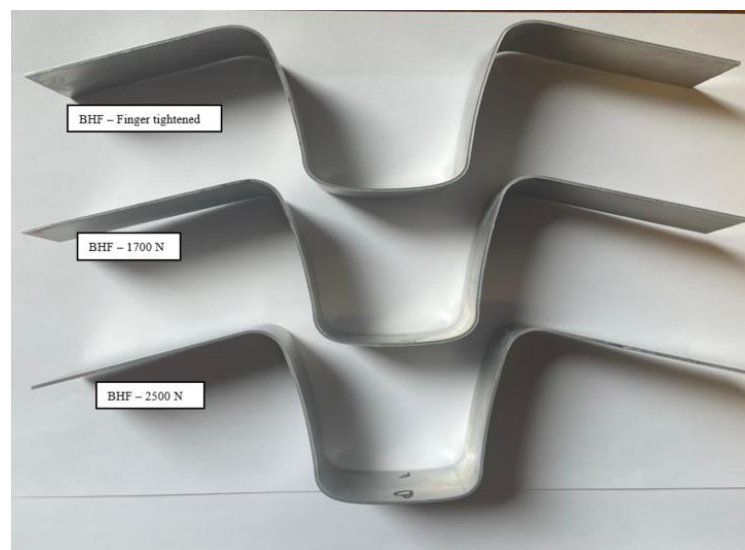


Figure 25. Profiles of Al/PP/Al specimens with 0.2/0.8/0.2 mm thickness combination after springback.

Figure 26 compares the load vs. punch displacement curves for laminates with 0.2/0.8/0.2 and 0.22/0.8/0.22 mm thickness combinations. Both experimental and simulated curves are shown. The load curves obtained from simulations are almost identical up to a punch displacement of 12 mm; this is the period where the material is made to wrap around the punch and die radius. At displacements higher than 12 mm, the load curves are similar in nature; the difference in their values can be attributed to the difference in the friction coefficients in the experiments and the simulations. Figure 27 shows the progression of U-channel forming along the punch load–displacement curve. The blank is being drawn into the die cavity at a punch displacement of around 26 mm. With increasing displacement, the load continues to increase slowly till the completion of drawing at 70 mm. Since the difference in total thickness of the specimens between Figure 26a,b is only 0.04 mm, the punch loads do not show any significant difference over the entire forming process of the U-channel.

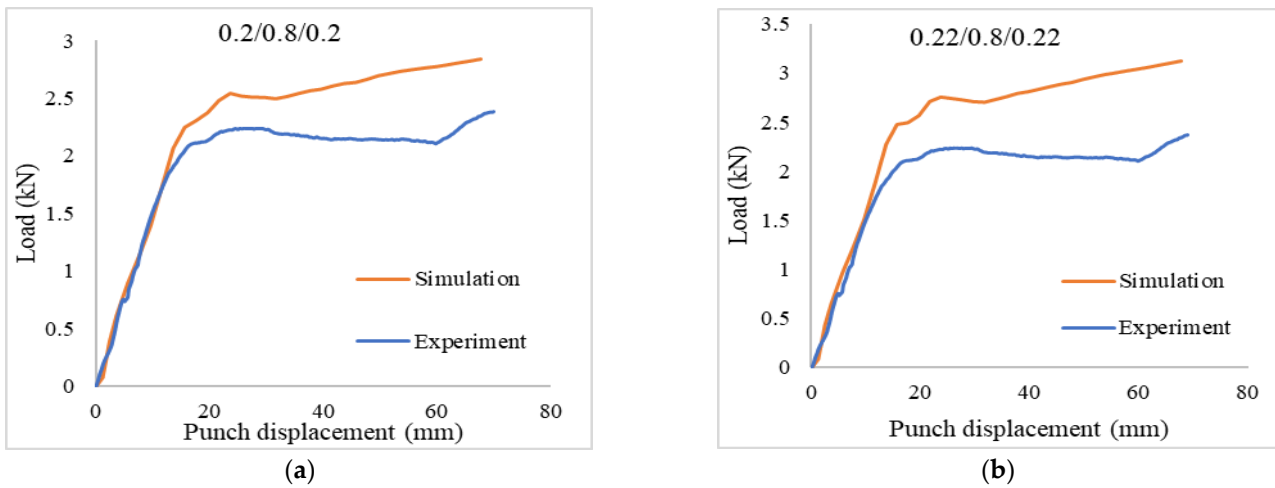


Figure 26. Comparison of load curves from experiment and simulation (a) 0.2/0.8/0.2 mm and (b) 0.22/0.8/0.22 mm thickness combinations.

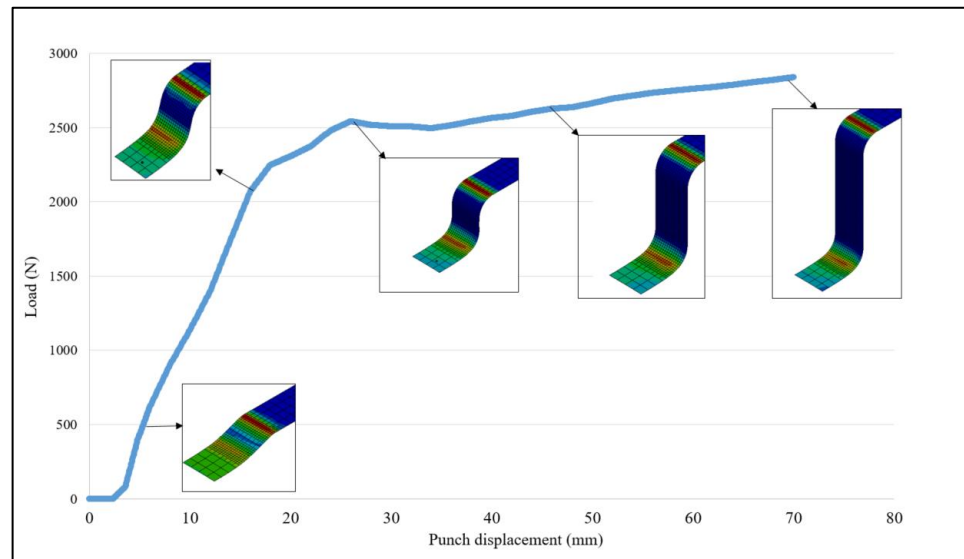


Figure 27. Stages of U-channel drawing along the punch load vs. displacement curve for the 0.2/0.8/0.2 mm sandwich laminate.

4. Conclusions

The springback behavior of aluminum-polypropylene-aluminum laminates under draw bending conditions is studied using finite element simulations of the forming of U-channels following the Numisheet’93 guidelines. The springback behavior of single aluminum sheets is also studied under similar conditions to make comparisons. The springback parameters considered are the wall angle, flange angle and radius of curvature of the wall of the U-channels.

In the study of single SA5182 (AA5182-O) sheets in the thickness range of 0.2 mm to 1.2 mm, it is seen that increasing the sheet thickness decreases the wall angle and increases both flange angle and radius of curvature of the wall, indicating that the springback behavior is improved. The Al/PP/Al sandwich laminate also shows lower wall angles, higher flange angles and higher radii of curvature of the wall with increase in laminate thickness. However, this is true up to a certain core thickness and then the laminate shows an increased springback behavior. When comparing a 1.2 mm thick SA5182/PP/SA5182 laminate with a thickness combination of 0.2/0.8/0.2 mm and a 1.2 mm thick single SA5182 sheet, the single aluminum sheet displays a better springback behavior for 8 mm die

and punch radius. This is because of the lower overall bending stiffness of the laminate compared to the single aluminum sheet.

The springback response of sandwich laminates is higher than that of the single aluminum sheet if they have the same thickness. For equal or better springback response, it may be required to adjust the core and skin thicknesses so that the bending stiffness of the sandwich laminate is higher than that of the single aluminum sheet. Based on the available design dimensions, a combination of skin and core thicknesses can be selected to show a better springback behavior along with lower overall weight of the laminate compared to a single sheet of aluminum.

A larger die radius can be used to reduce the springback of an Al/PP/Al sandwich laminate. Since the punch radius only has a positive effect on springback in the flange angle, it may be used as a factor to control springback in parts where the dimensional tolerance of the wall is high. The core thickness must be below a value of 1.6 mm to have reduced springback when using skins in the thickness range of 0.2 mm and 0.25 mm. The skin thickness can be increased to attain lower springback. The blank holder force (BHF) is varied between 500 and 2500 N for four thickness combinations. With increasing BHF, the wall angle increases, the flange angle first decreases and then increases, and the radius of curvature of the wall either decreases or remains the same. This indicates that BHF has a negative effect on the springback behavior of the sandwich laminates. The wall angle increases, and the flange angle decreases with increasing punch-die gap.

Author Contributions: Writing—review & editing, C.K.K. and P.K.M. All authors have read and agreed to the published version of the manuscript.

Funding: This research received no external funding.

Data Availability Statement: Not applicable.

Conflicts of Interest: The authors declare no conflict of interest.

References

1. Wagoner, R.H.; Lim, H.; Lee, M.G. Advanced Issues in springback. *Int. J. Plast.* **2013**, *45*, 3–20. [[CrossRef](#)]
2. Trzepieciński, T.; Lemu, H.G. Effect of Computational Parameters on Springback Prediction by Numerical Simulation. *Metals* **2017**, *7*, 380. [[CrossRef](#)]
3. Lee, J.-S.; Choi, S.-Y.; Lee, S.-K.; Song, J.-H.; Noh, W.; Choi, S.; Kim, G.-H. Roll forming process of automotive seat rail with 980 DP steel using Yoshida-Uemori kinematic hardening model. *Procedia Manuf.* **2018**, *15*, 796–803. [[CrossRef](#)]
4. Aerens, R.; Vorkov, V.; Duflou, J.R. Springback prediction and elasticity modulus variation. *Procedia Manuf.* **2019**, *29*, 185–192. [[CrossRef](#)]
5. Tang, B.; Lu, X.; Wang, Z.; Zhao, Z. Springback investigation of anisotropic aluminum alloy sheet with a mixed hardening rule and Barlat yield criteria in sheet metal forming. *Mater. Des.* **2010**, *31*, 2043–2050. [[CrossRef](#)]
6. Sumikawa, S.; Ishiwatari, A.; Hiramoto, J. Improvement of springback prediction accuracy by considering nonlinear elastoplastic behavior after stress reversal. *J. Mater. Process. Technol.* **2017**, *241*, 46–53. [[CrossRef](#)]
7. Hou, Y.; Min, J.; Lin, J.; Liu, Z.; Carsley, J.E.; Stoughton, T.B. Springback prediction of sheet metals using improved material models. *Procedia Eng.* **2017**, *207*, 173–178. [[CrossRef](#)]
8. Liu, J.; Liu, W.; Xue, W. Forming limit diagram prediction of AA5052/polyethylene/AA5052 sandwich sheets. *Mater. Des.* **2012**, *46*, 112–120. [[CrossRef](#)]
9. Harhash, M.; Gilbert, R.R.; Hartmann, S.; Palkowski, H. Experimental characterization, analytical and numerical investigations of metal/polymer/metal sandwich composites—Part 1: Deep drawing. *Compos. Struct.* **2018**, *202*, 1308–1321. [[CrossRef](#)]
10. Ferrari, F. Lightweight Metal/Polymer/Metal Sandwich Composites for Automotive Applications. Ph.D. Thesis, University of Windsor, Windsor, ON, Canada, 2017.
11. Wapande, S.H.; Elibol, C.; Konar, M. Effect of extruded low-density polyethylene on the microstructural and mechanical properties of hot-press produced 3105 aluminum composites. *Mater. Test.* **2021**, *63*, 34–40. [[CrossRef](#)]
12. Liu, L.; Wang, J. Modeling Springback of Metal-Polymer-Metal Laminates. *J. Manuf. Sci. Eng. Trans. ASME* **2004**, *126*, 599–604. [[CrossRef](#)]
13. Gardiner, F. The Springback of Metals. *Trans. ASME* **1957**, *79*, 1–9.
14. Ito, K.; Kasajima, M.; Furuya, S. Bending and springback theory of metal-polymer sandwich laminates. *J. Macromol. Sci. Part B Phys.* **1981**, *19*, 773–791. [[CrossRef](#)]
15. Harhash, M.; Gilbert, R.R.; Hartmann, S.; Palkowski, H. Experimental characterization, analytical and numerical investigations of metal/polymer/metal sandwich composites—Part 2: Free bending. *Compos. Struct.* **2020**, *232*, 111421. [[CrossRef](#)]

16. Liu, J.; Xue, W. Unconstrained bending and springback behaviors of aluminum-polymer sandwich sheets. *Int. J. Adv. Manuf. Technol.* **2016**, *91*, 1517–1529. [[CrossRef](#)]
17. Ahmed, R.O.; Chatti, S. Simplified springback prediction of thick sandwich panel. *J. Sandw. Struct. Mater.* **2018**, *22*, 1019–1038. [[CrossRef](#)]
18. Mohammadi, S.; Parsa, M.; Aghchai, A.J. Simplified springback prediction in Al/PP/Al sandwich air bending. *J. Sandw. Struct. Mater.* **2015**, *17*, 217–237. [[CrossRef](#)]
19. Parsa, M.H.; Nasher al ahkami, S.; Ettehad, M. Experimental and finite element study on the spring back of double curved aluminum/polypropylene/aluminum sandwich sheet. *Mater. Des.* **2010**, *31*, 4174–4183. [[CrossRef](#)]
20. Solfronk, P.; Sobotka, J.; Korecek, D. Effect of the Computational Model and Mesh Strategy on the Springback Prediction of the Sandwich Material. *Machines* **2022**, *10*, 114. [[CrossRef](#)]
21. Keipour, S.; Gerdooei, M. Springback behavior of fiber metal laminates in hat-shaped draw bending process: Experimental and numerical evaluation. *Int. J. Adv. Manuf. Technol.* **2019**, *100*, 1755–1765. [[CrossRef](#)]
22. Aghchai, A.J.; Abolghasemi, A.; Moradkhani, B.; Tajik, M. Experimental, theoretical and numerical investigation of springback behavior of Al/composite/Al sandwich sheet. *J. Sandw. Struct. Mater.* **2017**, *19*, 659–678. [[CrossRef](#)]
23. Stoughton, T.B.; Shi, M.F.; Huang, G.; Yoon, J.W. Material characterizations for Benchmark 1 and Benchmark 2. In *NUMISHEET 2014: The 9th International Conference and Workshop on Numerical Simulation of 3D Sheet Metal Forming Processes*; AIP Publishing: Melville, NY, USA, 2014. [[CrossRef](#)]
24. LS-DYNA. MAT226_AA5182-O_NUMI2014. In *LS-DYNA Material Library*; Livermore Software Technology Corporation: Livermore, CA, USA, 2014.
25. Banabic, D. *Sheet Metal Forming Processes Constitutive Modelling and Numerical Simulation*; Springer: Berlin/Heidelberg, Germany, 2010.
26. Smith, L.M. NUMISHEET 2005: Proceedings of the 6th International Conference and Workshop on Numerical Simulation of 3D Sheet Metal Forming Process. In *AIP Conference Proceedings*; American Institute of Physics: Detroit, MI, USA, 2005.
27. Zhou, Y.; Mallick, P.K. Effects of temperature and strain rate on the tensile behavior of unfilled and talc-filled polypropylene. Part I: Experiments. *Polym. Eng. Sci.* **2002**, *42*, 2449–2460. [[CrossRef](#)]
28. Makinouchi, A. *NUMISHEET '93: Proceedings of the 2nd International Conference of Numerical Simulation of 3-D Sheet Metal Forming Processes; Verification of Simulation with Experiment*; Elsevier: Isehara, Japan, 1993.
29. Maker, B.; Zhu, X. *Input Parameters for Springback Simulation Using LS-DYNA*; Livermore Software Technology Corporation: Livermore, CA, USA, 2001.
30. Mallick, P.K. *Fiber Reinforced Composites Materials, Manufacturing and Design*, 3rd ed.; Taylor & Francis Group, LLC: Boca Raton, FL, USA, 2007.
31. Chirita, B.A. Factors of influence on the springback of formed metal sheets. In *Proceedings of the ESAFORM—The 5th International Conference on Material Forming, Krakow, Poland, 14–17 August 2002*.
32. Stein, J.J. The Effect of Process Variables on Sheet Metal Springback. In *International Body Engineering Conference and Exposition*; SAE International: Detroit, MI, USA, 1998. [[CrossRef](#)]
33. Tong, V.-C.; Nguyen, D.-T. A study on spring-back in U-draw bending of DP350 high-strength steel sheets based on combined isotropic and kinematic hardening laws. *Adv. Mech. Eng.* **2018**, *10*, 1687814018797436. [[CrossRef](#)]
34. Kadkhodayan, M.; Zafarparandeh, I. An investigation into the influence of blankholder force on springback in U-bending. *Arch. Metall. Mater.* **2009**, *54*, 1183–1190.